IEEE Journal of Translational Engineering in Health and Medicine

Received 26 September 2023; revised 2 September 2024; accepted 17 September 2024.
Date of publication 1 October 2024; date of current version 29 October 2024.

Digital Object Identifier 10.1109/JTEHM.2024.3471468

A Novel Chest-Based PPG Measurement System

QIUYANG LIN[1], (Member, IEEE), HAOCUN WANG[2], DWAIPAYAN BISWAS[1], (Member, IEEE), ZHEYI LI[1,3], (Member, IEEE), ERIKA LUTIN[1,3], CHRIS VAN HOOF[1,3], (Member, IEEE), MINGYI CHEN[2], (Senior Member, IEEE), AND NICK VAN HELLEPUTTE[1], (Member, IEEE)

[1]imec, 3001 Heverlee, Belgium
[2]School of Micro-Nano Electronics, Shanghai Jiaotong University, Shanghai 200240, China
[3]Department of ESAT, Katholieke Universiteit Leuven, 3001 Heverlee, Belgium

CORRESPONDING AUTHOR: M. CHEN (mychen@sjtu.edu.cn)

This work was supported by the National Natural Science Foundation of China under Grant 62174109.

ABSTRACT Advancements in integrated circuit (IC) technology have accelerated the miniaturization of body-worn sensors and systems, enabling long-term health monitoring. Wearable electrocardiogram (ECG), finger photoplethysmogram (PPG), and wrist-worn PPG have shown great success and significantly improved life quality. Chest-based PPG has the potential to extract multiple vital signs but requires ultra-high dynamic range (DR) IC to read out the small PPG signal among large respiration and artifacts inherent in daily life. This paper presents a dedicated high DR system for wearable chest PPG applications with a small form factor. The whole measurement system is integrated on a 20 cm^2 PCB board. We have formulated a comprehensive evaluation protocol to validate the system with on-body chest PPG measurement in the workspace environment. First, chest PPG data was obtained from 6 adults and compared to data from a standard ECG patch. This system showed an average absolute deviation (AD) of 0.41 beats per minute, achieving $>$ 99.53% heart rate (HR) accuracy. Second, chest PPG was recorded and compared to conventional PPG finger clip and PPG wristband, also showing $>$ 98.6% HR matching and an absolute deviation in the standard deviation of NN intervals (SDNN) of $<$12.8 ms for HRV monitoring within the protocol. Moreover, it successfully derives other vital parameters such as respiration rate and blood oxygen level (SpO_2), showing the advancement among all these three reference modalities. This system can pave the way for new application areas, such as chest patches, to monitor chronic heart and respiratory diseases.

INDEX TERMS Chest photoplethysmogram (PPG), dynamic range (DR), electrocardiogram (ECG), blood oxygen level (SpO_2), respiration.

Clinical and Translational Impact Statement—We developed the high dynamic range chest PPG readout system, benchmarking the measurement results with other conventional devices. Thus, our approach could provide patients with vital signs recordings (HR, HRV, SPO2, Respiration) with improved comfortability and high accuracy, aiming for pulmonary disease and general monitoring.

I. INTRODUCTION

HEART and respiratory diseases are two major causes of death globally [1], alerting people to pay more attention to fitness and wellness monitoring. Modern digital technologies such as smartphones and wearable sensors have gained significant momentum in healthcare since they enable long-term and ambulant monitoring. To obtain heart rate (HR) and heart rate variability (HRV), an electrocardiogram (ECG) is considered the gold standard. It allows the monitoring of abnormal signals for people with chronic cardiac conditions [2], [3], [4], [5]. The primary focus of the last two decades has been making reliable wearable chest ECG sensors with a small form factor and low cost (Fig. 1(a)) [6], [7], [8], [9], [10], [11], [12]. However, some problems remain for ECG sensors, such as the fast degradation of the electrodes, uncomfortable gel, and measurement challenges caused by electrode offset, saturation, and noise [8], [11], [12], [13], [14].

Photoplethysmogram (PPG) is an optical monitoring method frequently used in clinical settings such as PPG finger clips. With the miniaturized sensors (emitters and detectors), PPG has nowadays become a popular alternative to ECG. Integrated into a wrist-worn watch/band (Fig. 1(b)), it can extract not only HR and HRV but also the blood oxygen level

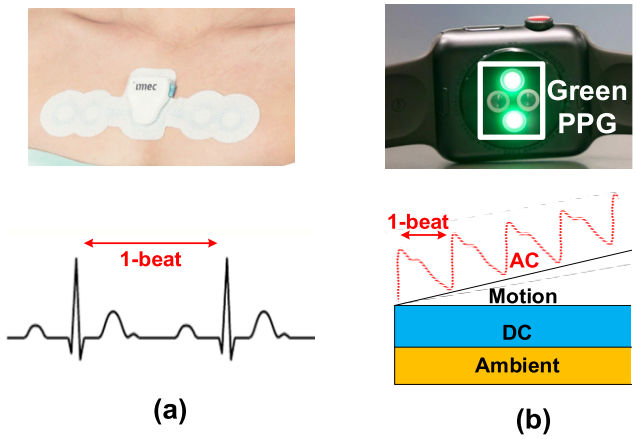

FIGURE 1. (a) A wearable ECG patch and a standard ECG signal (b) A wearable PPG watch and a standard PPG signal.

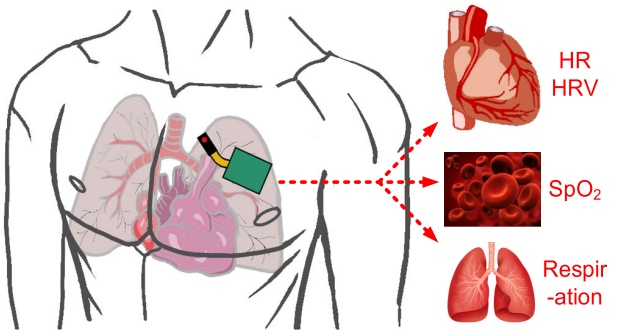

FIGURE 2. Respiratory monitoring metrics using chest PPG.

(SpO_2) [15], [16], [17], [18], [19], which is a key parameter for respiratory diseases [20], [21].

The physics behind PPG monitoring is based on Diffuse Optical Imaging (DOI). Light can scatter through strongly turbid materials such as human tissue with a probability density function pattern when the scattering coefficient is much higher than the absorption coefficient [22]. Beer-Lambert Law states that the absorbance of light (A) is linearly proportional to the concentration (c), the molar absorption coefficient (ε), and the optical path length (l) [23], [24], as shown in equation (1).

$$A = \varepsilon c l \tag{1}$$

The main chromophores inside the blood, like oxyhemoglobin (Hb) and deoxyhemoglobin (HbO_2), absorb near-infrared light, varying with blood volume changes caused by heartbeats. The PPG can be obtained with known absorption and a fixed distance by measuring the received light. Consequently, HR and HRV can be calculated. Moreover, employing two different wavelengths makes it possible to determine the absolute concentration of Hb/HbO_2, which in turn allows for deriving SpO_2 [25], [26], [27].

The pulsatile part (Fig. 1(b)) (AC component) only takes up a small portion of the total received light. This pulsatile AC component is superimposed on a large DC component. The latter is related to static light absorption and scattering in tissues like bones, skin, and muscle [27]. The AC/DC ratio also called the perfusion index (PI), is usually less than 5% on the finger and can drop to as low as 0.5% on the wrist [20], [28]. Measurement setup (LED/PD shielding and contact with the skin) results in large variations in the PI. Hence, a high dynamic range (DR > 80 dB) readout chip is needed to ensure accurate HR recording [29], [30], [31], [32], [33]. However, the situation is more difficult under ambulatory conditions. PPG is notoriously susceptible to motion artifacts inherent in daily life [34]. Especially on the finger/wrist, where large and unpredictable movements occur, PPG sensing can be unreliable.

The chest (Fig. 2) is usually less subject to motion than the finger/wrist. Thus, it could potentially solve the problems mentioned above. However, chest PPG has not been well studied due to hardware limitations. Based on our prior work [32], we aim to build a chest PPG system and explore the quality and performance of chest PPG signals in this manuscript. More specifically, we aim to validate chest PPG against the gold standard, i.e., ECG, and benchmark the performance against finger PPG and wrist-worn PPG on human subjects.

The rest of the paper is organized as follows. Section I describes the motivation and the problem formulation to do PPG sensing on the chest. Section III shows the proposed methodology, detailed experimental protocols, and the algorithms to extract the desired biomedical parameters. Section IV presents the measurement results and the analysis. Section V draws the conclusion.

II. MOTIVATION AND PROBLEM FORMULATION

As discussed previously, chest ECG monitoring is the gold standard for accurate HR extraction, while finger PPG is essential for deriving SpO_2 in clinical settings [14]. However, two individual systems are required if both bio-parameters need to be monitored consistently. Chest PPG is a promising candidate to provide both metrics in a single small form factor device. By placing the PPG sensor on the chest, the HR and SpO_2 signal can be derived together with the respiration signal. Many studies have attempted to obtain HR and SpO_2 from the chest. However, none have succeeded [35], [36], [37], [38], [39] without a high DR readout chip.

Another advantage of chest PPG over finger PPG is the potential to measure the respiration rate [35], [39], which is useful for heart and respiratory diseases [37], sleep or apnea monitoring [38], and fitness monitoring [35], [36], [37], [38], [39]. It is worth noting that severe COVID-19 cases can show a SpO_2 level consistently lower than 90% with fast respiration and HR [21], [40], making chest PPG a potentially interesting candidate for COVID-19 monitoring. A chest PPG sensor embedded in a small form factor patch also provides a mechanically more robust connection to the skin than a wristwatch, easing the motion artifact removal procedure. The working principle behind extracting respiration from the

IEEE Journal of Translational Engineering in Health and Medicine

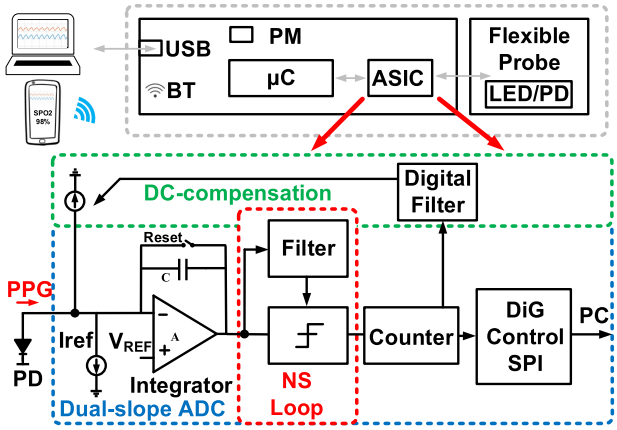

FIGURE 3. The proposed wearable chest PPG monitoring system with the chest PPG monitoring ASIC block and flexible LED/PD. The system can communicate to PC/Smart Phone by USB. The ASIC is implemented with TSMC 180 nm and can readout PPG signal from the PD.

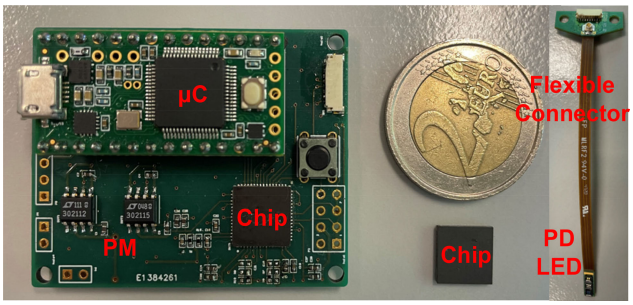

FIGURE 4. The chest PPG system prototype with a size of 5 cm × 4 cm, the flexible probe.

chest differs from measuring HR. When large respiration (10X > AC) is introduced, the light path can be changed due to breathing, and the PPG signal can be primarily modulated by respiration [41]. This results in a low-frequency, high-amplitude AC signal superimposed on a conventional PPG signal [42]. The respiration signal can be extracted with suitable bandpass filtering.

The primary bottleneck for chest PPG modality adoption is the lack of high DR in PPG ASICs. As introduced previously, respiration can lead to a large amplitude modulation in the PPG signal. Thus, an extra 20 dB is needed compared with wrist PPG extraction. This, along with an extremely low PI on the chest, poses a very stringent DR requirement (>100 dB) for readout circuitry [32], [42].

III. METHODS

A. SET-UP

We previously developed a dedicated high DR readout ASIC (Fig. 3) [42]. This chip applies a novel noise shaping (NS) slope architecture and achieves a maximum of 134 dB DR within the PPG bandwidth (0.5-20 Hz), which is the highest compared with the state-of-the-art works [31], [43], [44] and makes it attractive for chest PPG applications. The chip occupies 8.4 mm^2, manufactured in TSMC 180 nm technology, with a power consumption of 28 μW/channel, which is reasonable in PPG application. Together with the LED power consumption, this chip consumes a total power of 333 μW. For a conventional button cell with a 50 mAh capacity, this chip can operate around 150 hours (6 days). It was suitable for chest PPG applications [42].

In this manuscript, we evaluated the chest PPG performance in realistic scenarios and benchmarked it against other systems to this end. We created a system demonstrator based on the ASIC, as shown in Fig. 3, in which an onboard microcontroller is used with wired/wireless connections to a PC or other mobile devices to establish the communication interface. Power management (PM) modules are used to ensure robust supply voltage for the ASIC. Furthermore, we implemented a flexible sensor probe separately from the electronics to explore different probe positioning easily. At the same time, we also built the software with algorithms developed to obtain and process the chest PPG signal. The PPG acquisition system is shown in Fig. 4. Since the purpose was to evaluate the performance in a real-life scenario, we aimed for a reasonably small board to minimize cable artifacts. However, absolute miniaturization was not the aim of this work. The total board area can be easily reduced by 5x by eliminating test points and using smaller SMD components.

Conventional PPG measurement locations are well-defined, e.g., on the fingertip or the wrist. Most often, the reflection mode PPG is applied, where both LED and PD are used on the same side with a higher signal amplitude than the transmission mode PPG. Our chest PPG system also employs the reflection mode with red light (660 nm) and infrared light (950 nm) to be the light source generated from OSRAM SHF7060 LED [45]. The LED drivers are also on the chip. Compared to green light, as used in the state-of-the-art PPG system, red light and infrared light have a longer wavelength, resulting in a larger penetration depth towards the tissue. This is more suitable for chest PPG monitoring since the blood vessels on the chest are usually covered by thick muscles. However, the chest has a large area. It is essential to figure out a good measurement location for chest PPG extraction. Therefore, we first measured the PPG signal at different locations on the chest and compared it with the standard PPG waveform format to find out the best location for PPG extraction [30]. We divided the chest areas into four parts, i.e., upper/lower anterior areas and upper/lower lateral areas. The sampling rate was 1024 Hz and LED applied a 24 mA peak current with a 1% duty cycle to save power. Currently, the Bluetooth option has not been implemented yet on the board.

B. EXPERIMENTAL PROTOCOL

We conducted three measurements on ten subjects of different genders and skin types to evaluate how accurate chest PPG is in extracting bio-parameters compared with the standard wearable devices (ECG, finger PPG, and wrist PPG) in a controlled ambulant environment. To evaluate the

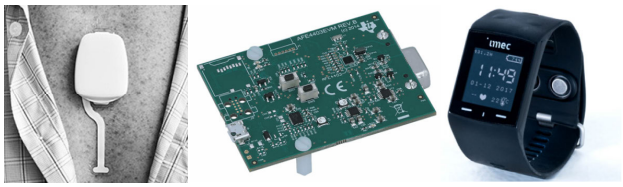

FIGURE 5. (a) IMEC 3-channel ECG patch. (b) TI 4403 PPG evaluation module. (c) IMEC Chill+ wrist module.

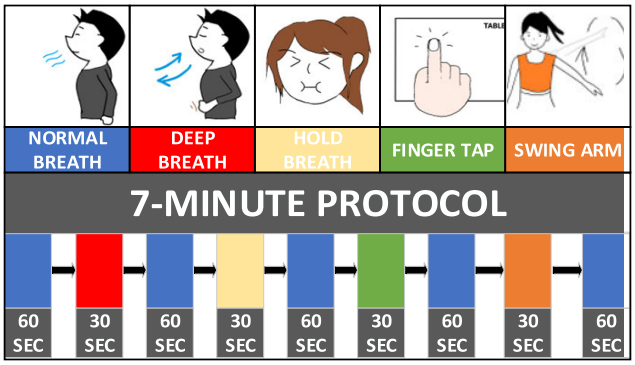

FIGURE 6. A 7-minute experimental protocol comprising: normal breath, deep breath, hold breath, finger tap and swing arm phases.

performance of the recorded chest PPG, we used 3 reference systems. We used a custom-built chest ECG (Fig. 5(a)) as the reference. We also compared finger-clip PPG (recorded with an example state-of-the-art Orsam SFH7050 LED and PD module with TI AFE 4403 PPG evaluation system (Fig. 5(b)) and wrist PPG using a custom-built wristwatch [34] which allows us to capture raw PPG signals [46] (Fig 5 (c)).

All activities were performed in a voluntary manner. A custom experiment protocol was designed that could be performed in seated scenarios in an ambulant workspace environment, thereby ensuring a high degree of motion artifacts in the chest PPG signal acquisition. Our experiment comprises data collected from different subjects (different ethnic backgrounds), male/female, ages ranging from 25-40, with their informed consent, in a natural office environment (Due to the wire connections). The subjects were asked to do a series of activities in a sequence to represent motions inherent in a seated workplace environment (Fig. 6). In this protocol, the subjects performed four activities. First, the subjects performed 60 s of normal and 30 s of deep breathing in an office chair. Second, all subjects were required to do 60 s of normal breathing followed by 30 s of holding their breath. To evaluate the system with hand movements. All subjects needed to use their finger to tap the table with a speed of around 1 tap/second. Last, after 60 s of normal breathing, all subjects needed to perform intense arm swing movements for another 30 s. Before the end of the protocol, the subjects were asked to do 60 s of normal breathing. We envisage this protocol will enable benchmarking of the proposed chest PPG measurement modality under three diverse scenarios: 1) explore the optimal location for chest PPG acquisition; 2) comparison with conventional chest ECG; 3) comparison with wrist/finger PPG during seated workplace activities. Although data acquisition was carried out in a seated position, participants were encouraged to carry out tasks in a voluntary manner, ensuring maximal variability in the underlying data. The primary idea of this protocol was to capture a baseline for this proof-of-concept chest-based acquisition system.

In our first experiment, we validated our chest PPG system against chest ECG since ECG is considered the gold standard for HR and HRV monitoring. Subjects 1-6 volunteered to join the experiments, including 4 male subjects and 2 female subjects, of age range 25-35 and different ethnic backgrounds, with their informed consent. The LED/PD soft patch of our chest PPG system was attached to the upper anterior areas of the subjects with black tape. We applied the IMEC 3-channel ECG patch (Fig. 5(a)) for reference. To avoid gel degradation during experiments, disposable wet-gel electrodes were used. These patches were also placed on the anterior areas of the subjects and stored the data in their flash memory. It should be noted that we used two different platforms to measure the PPG and ECG signals. To enable a direct comparison, the platforms needed to be synchronized in real time. Therefore, the subjects simultaneously tapped the ECG patch and chest PPG probe. This tap could then serve as a synchronization marker to align the signals in the time domain.

Similarly, in the second experiment, we validated our chest PPG system to get HR, HRV and compared them with the commercial TI 4403 evaluation board. 10 subjects (1-10, 6 males, 4 females, between the age range 25-43 and different ethnic backgrounds, with their informed consent.) participated in this experiment. The TI 4403 has a flexible LED/PD sensor that can be taped to the right-hand fingertip. The synchronization mark is generated using a right-hand finger to tap the chest PPG probe. Then, a noticeable spike can be seen from the transient waveform.

In the third experiment, we compared our chest PPG system to the IMEC Chill+ PPG wristband. We applied the wristband to the left wrist of the subjects. Also, all subjects (1-10, 6 males, 4 females) participated in this experiment.

C. DATA PROCESSING

As discussed in the set-up description, the real-time PPG/ECG data from the four chest locations were recorded. Before analyzing the data, time-domain synchronization was applied. Thereafter, the data were processed with a main focus on the extraction of HR, HRV, and respiration. Unlike SpO_2, which can only be obtained via PPG, HR, and HRV can be obtained via both PPG and ECG. In a standard PPG waveform, each heartbeat cycle contains only one systolic peak [29]. Thus, the HR can be recorded by detecting the PPG's systolic peaks. Meanwhile, the HRV can be calculated by measuring the variation between the systolic peaks.

IEEE Journal of Translational Engineering in Health and Medicine

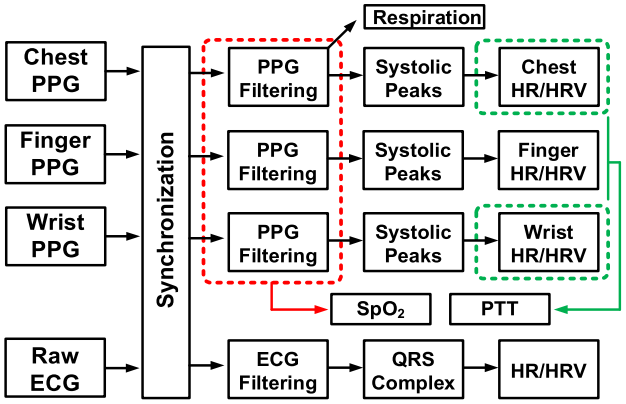

FIGURE 7. Overview of the signal processing methodology adopted for the analysis.

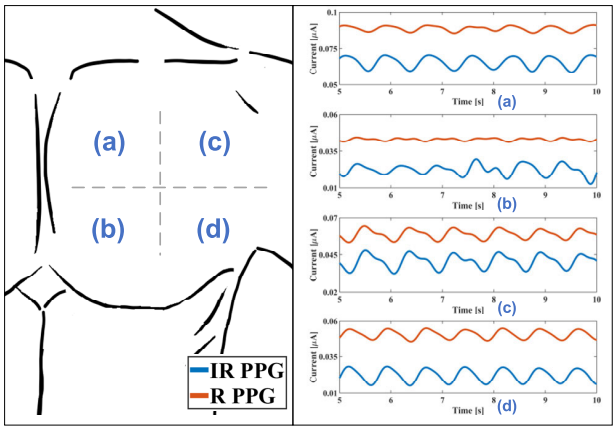

FIGURE 8. Four chest PPG area, roughly classified by a rectanglar shape [54]: (a) upper lateral area (b) lower lateral area (c) upper anterior area (d) lower anterior area, and the corresponding PPG waveforms.

Similarly, for an ECG signal, each heartbeat cycle comprises only one QRS complex. By detecting the amount of variation in QRS complexes, the HR and HRV can be extracted from ECG monitoring [47].

The signal processing procedures are illustrated in Fig. 7. Low-pass filters (with 5 Hz cut-off frequency and 60 dB attenuation) filtered the raw PPG/ECG data sets to get rid of the out-of-band noise since the sampling frequency of the system is 1024 Hz. Then, we used the Heartpy algorithm [48] to extract the systolic peaks and QRS complex. A short-time window with a moving average was applied to mark possible regions (of a small number of samples) in which peaks could appear. Thereafter, the highest values were selected to be peaks. The accuracy of the peak detection is reported to be 99.72% [48]. Following the peak detection, the HR and HRV were obtained.

The most straightforward way to evaluate HR is by calculating the beats per minute (bpm) and comparing the result to a ground truth reference. In ECG signal analysis, the peak-to-peak (RR) interval is used to present the time difference between two heartbeats. After filtering out the artifact and noise, the interval is then called the NN interval [48], [49]. This can also be applied to PPG monitoring. As a result, to evaluate HRV, the standard deviation of NN intervals (SDNN) is usually used [50], [51], [52]. Therefore, it can be represented as:

$$SDNN = \sqrt{\frac{1}{N-1}\sum_{i=1}^{N}(NN_i - \overline{NN})^2} \tag{2}$$

To evaluate the HR(V) recording accuracy, we introduced the Absolute Difference (AD) and Relative Difference (RD), which are defined as:

$$AD_i = \left|HR_{mea}(i) - HR_{ref}(i)\right| \tag{3}$$

$$RD_i = \frac{AD_i}{\left|HR_{ref}\ (i)\right|} \times 100\% \tag{4}$$

where HR_{mea}(i) and HR_{ref}(i) are the HR value of measured data and the reference data of the i-th subject, respectively.

It is worth noting that these two equations can be applied to both HR and SDNN of HRV. It is important to note we have interchangeably referred to HRV in this paper.

As introduced previously, other than HR and HRV, PPG monitoring can also provide SpO_2 information, which is essential in pulmonary applications. SpO_2 is derived from dual-light measurement, red (R) and infrared (IR), as follows [53]:

$$\%SpO_2 = a - b * P \tag{5}$$

where P is the perfusion index ratio of two PPG responses. The variables a and b are constants based on measurement setup [53]. One of the advantages of chest PPG is that respiration can be extracted simultaneously as a large DC drift since the respiration rate has less frequency (< 0.5Hz) than the PPG signal (1-5 Hz bandpass filter can be used). By applying a low-pass filter (< 0.5 Hz cut-off frequency), respiration data can be obtained.

IV. RESULTS AND DISCUSSION

A. MEASUREMENT LOCATION

As shown in Fig. 8, subjects were measured in different locations. Due to the advancement of the system, the chest PPG signals were extracted successfully in all four areas. However, the upper anterior showed a more standard PPG waveform morphology-wise [30]. This could be due to the fact that we have more adipose on the low anterior and lateral chest, increasing the distance that LED light travels to reach the blood vessels [54]. As a result, we chose the upper anterior area as a fixed location for chest PPG exploration to minimize the experimental difference. It is important to note that we ensured maximal coverage of the chest area while performing the acquisition. We envisage this study will present an engineering perspective and help to augment the clinical decision-making process with respect to the sensing position for chest-based PPG.

TABLE 1. HR and HRV Analysis in chest PPG vs. chest ECG experiment.

	HR Analysis					AD_{SDNN} Analysis (HRV)				
Subjects	Chest PPG (bpm)	Chest ECG (bpm)	AD_{HR} (bpm)	RD_{HR} (%)	All time (ms)	Normal Breath (ms)	Deep Breath (ms)	Hold Breath (ms)	Finger Tap (ms)	Swing Arm (ms)
1	84.54	84.52	0.02	0.02	7.23	4.05	11.78	1.51	8.37	61.17
2	78.43	78.14	0.29	0.37	30.02	19.55	33.37	20.08	33.55	64.04
3	90.74	91.37	0.63	0.69	8.58	10.31	46.16	12.41	15.15	44.5
4	90.09	90.23	0.14	0.16	12.27	7.44	20.39	4.46	13.61	59.17
5	87.04	87.54	0.50	0.57	27.9	17.87	34.69	9.28	31.9	76.68
6	90.95	91.85	0.90	0.98	31.61	10.82	73.15	9.17	30.61	31.17
Average			0.41	0.47	19.60	11.67	36.59	9.49	22.20	56.12
Median			0.39	0.47	20.10	10.57	34.03	9.23	22.88	60.17

B. CHEST PPG VS CHEST ECG EXPERIMENT

Six subjects participated in the first experiment, comparing chest PPG with ECG. Chest PPG patches were placed onto the six subjects' upper anterior chest area, and ECG patches were located in the same areas. Next, the subjects were requested to follow the experimental protocol. Fig. 9 (a) shows samples of both chest PPG and chest ECG, after time domain synchronization during the first two actions of the protocol: normal and deep breathing. The baseline current is stable when the subject breathes normally. Then, there is a baseline vibration during the deep breathing period. The pulsatile PPG signal is invisible since the baseline current is too big. However, after filtering out the DC value by a bandpass filter (1-5 Hz), a clean chest PPG signal can be observed (Fig. 9(b)) during the normal breathing period. The systolic and diastolic peaks are evident and match the ECG signal beat-to-beat. During deep breathing, the PPG signal is modulated by respiration. Breathing changes the light path's length and the related signal amplitude. Luckily, the normal respiration rate (< 0.5 Hz) is much lower than the PPG signal frequency. It can be extracted by adding a low-pass filter. As seen from Fig. 9(c), each respiration cycle takes around 5 seconds, which matches well with the empirical value.

Table 1 shows the recording data of all 6 subjects. The first part of this table shows the chest PPG HR accuracy over a 7-minute recording period. The AD of the HR is at most 0.9 beat/min for all these 6 subjects compared to the reference ECG signal. And the relative deviation (RD) is less than 1%. Furthermore, the average and median AD and RD values show that the overall measurement accuracy is 99.5%, far beyond the maximum allowable HR error (10% or $\pm$5 bpm) used in hospital settings [55].

For HRV evaluation, we analyzed the chest PPG data based on the performed activities to understand the influence of motion artifacts on the acquired signal. It is worth noting that the chest ECG patch uses wet gel electrodes and can be considered a reliable reference during the measurement. The AD values of SDNN for the six subjects' chest PPG/ECG data were calculated. It can be seen that the average and median AD of SDNN in the complete protocol data collection are

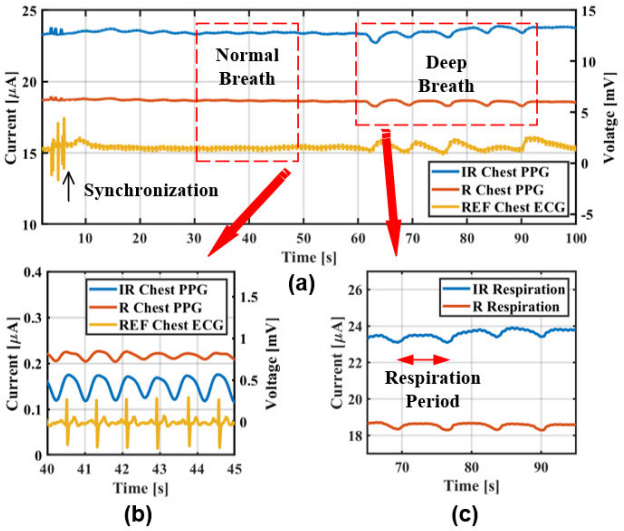

FIGURE 9. (a) A sample chest PPG/ECG measurement results; (b)Band-pass filtered chest PPG/ECG signals in normal breathing period; (c)Low-pass filtered respiration rates.

under 30 ms (19.6 ms and 20.1 ms, respectively). The smallest AD was obtained during the holding breath period, while the largest AD was recorded during the swinging arm activity, which involved large motion artifacts. The latter confirms that motion artifacts influence the chest PPG recording accuracy. However, chest PPG is still acceptable since the maximum AD of SDNN is 76.88 ms. Compared with the normal HR of 30-200 bpm (300 ms to 2000 ms), the error is much less than one heartbeat period [55]. In comparison to the golden reference (ECG), chest PPG shows high measurement accuracy in both HR and HRV.

C. CHEST PPG VS FINGER PPG EXPERIMENT

Ten subjects participated in a second experiment to benchmark the chest PPG against a commercial finger PPG module. We placed the commercial finger PPG module (TI 4403) on the left index finger of the subjects. Subsequently, the subjects were requested to follow the 7-mins protocol. Similar to the first experiment, the first step of data processing was

TABLE 2. HR and HRV Analysis in chest PPG vs finger PPG experiment.

	HR Analysis					AD_{SDNN} Analysis (HRV)				
Subjects	Chest PPG (bpm)	Wrist PPG (bpm)	AD_{HR} (bpm)	RD_{HR} (%)	All time (ms)	Normal Breath (ms)	Deep Breath (ms)	Hold Breath (ms)	Finger Tap (ms)	Swing Arm (ms)
1	76.46	77.28	0.82	1.06	7.8	5.52	13.09	5.1	160.3	36.84
2	77.71	78.88	1.17	1.48	19.97	33.86	72.73	41.94	42.42	67.72
3	80.78	78.33	2.45	3.13	16.03	16.5	28.3	12.71	0.71	107.28
4	76.85	76.74	0.11	0.14	10.6	22.68	22.68	5.38	41.91	30.75
5	87.57	89.61	2.04	2.28	0.42	5.07	11.7	17.84	29.1	14.89
6	79.06	80.06	1	1.25	20.05	13.32	2.62	31.8	33.83	203.06
7	68.6	69.24	0.64	0.92	25.68	34.41	64.27	14.01	11.34	79.31
8	77.72	77.86	0.14	0.18	5.61	1.64	5.66	32.35	50.65	20.59
9	72.88	72.89	0.01	0.01	3.21	5.15	36.39	9.07	104.71	51.34
10	75.83	75.83	0	0	18.6	27.25	7.56	41.55	4.54	37.12
Average			0.84	1.05	12.80	16.54	26.50	21.18	47.95	64.89
Median			0.73	0.99	13.32	14.91	17.89	15.93	37.87	44.23

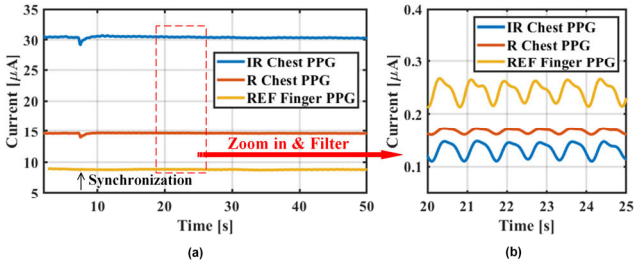

FIGURE 10. (a) A sample chest/finger PPG measurement results; (b) Band-pass filtered chest/finger PPG in normal breathing period.

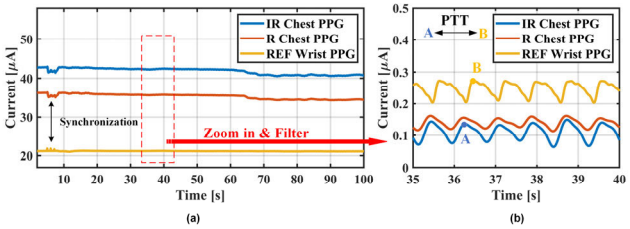

FIGURE 11. (a) Chest PPG and wrist PPG signals; (b) Band-pass filtered chest/wrist PPG in normal breathing period.

synchronizing between the two recording systems, as shown in Fig. 10(a). A bandpass filter (1-5 Hz) was applied to filter out the large DC and the out-of-band noise. Fig. 10(b) illustrates that three PPG waveforms are clear and match well in the time domain.

Again, we compared HR and HRV between chest PPG and reference finger PPG. The deviations in HR and HRV are presented in Table 2. In the HR analysis part, we measured the bpm of ten subjects based on chest PPG and finger PPG data and calculated the AD and RD values. The average AD was 0.84 bpm, and the average RD was 1.05%, which means that the HR acquired by chest PPG shows > 98.95% accuracy compared with finger PPG modality. Meanwhile, the SpO_2 can be extracted from both the chest and finger area with equation (5), showing a good matching with a maximum 3% difference, which is slightly larger than the commercial oximeter.

As for the HRV analysis part, the maximum relative error happened when subjects were swinging their arm. In this situation, both finger PPG and chest PPG were affected by large motion artifacts. The average AD of SDNN during arm swinging was 64.89 ms (with a maximum AD of 203.06 ms in subject 6). During the finger tapping period, the average AD of SDNN was 47.95 ms, which is > 2X larger than the one reported in Table 1, in which chest ECG was the reference. Possibly, finger tapping injects large motion artifacts into finger PPG but does not influence chest PPG. Moreover, the other 3 activities (holding breath/normal breathing/deep breathing) show similar low-level AD/RD values. The smallest AD/RD was obtained by averaging all 7-mins data. It means the chest PPG shows a high accuracy in long-time monitoring compared with the finger PPG modality.

D. CHEST PPG VS WRIST PPG EXPERIMENT

Lastly, ten subjects participated in a third experiment to benchmark the chest PPG against a wrist PPG module. As described before, we used the IMEC Chill+ watch as a reference and placed it on the subjects' left wrists. Again, the measurements started only after synchronization. Fig 11(a) shows a data segment of 100 s from one subject. Since both chest and wrist PPG are small, they need to be filtered and zoomed in to observe the details (Fig. 11 (b)). Both three PPG waves are clear with systolic/diastolic peaks. It is interesting to see I/IR chest PPG aligns well. Despite this, there is a time delay between chest PPG and wrist PPG. A and B are two systolic peaks from IR chest PPG and wrist PPG from the same HR cycle, respectively.

The AD and RD of HR are calculated in Table 3. The average AD of HR is 0.99 bpm, resulting in 1.31% RD. Thus, the average HR monitoring accuracy of chest PPG is > 98.6% when taking wrist PPG as the reference. For the HRV analysis part, the largest AD of SDNN was observed when the subjects were required to tap their finger, resulting in large motion artifacts. The smallest AD was recorded when the subject was breathing normally. At the same time, the average 7-mins

TABLE 3. HR and HRV Analysis in chest PPG vs wrist PPG experiment.

	HR Analysis					AD_{SDNN} Analysis (HRV)				
Subjects	Chest PPG (bpm)	Wrist PPG (bpm)	AD_{HR} (bpm)	RD_{HR} (%)	All time (ms)	Normal Breath (ms)	Deep Breath (ms)	Hold Breath (ms)	Finger Tap (ms)	Swing Arm (ms)
1	68.6	69.91	1.31	1.87	9.96	14.07	27.56	11.38	98.37	0.65
2	70.82	71.76	0.94	1.3	28.21	2.91	39.5	22.76	48.46	37.66
3	75.7	74.97	0.73	0.97	9.83	11.38	43.94	15.32	90.81	51.98
4	80.77	80.69	0.08	0.1	3.06	9.49	39	27.74	94.63	18.42
5	78.89	79.57	0.68	0.85	20.76	1.56	44.17	36.69	90.5	26.84
6	74.94	76.29	1.35	1.77	2.75	16.83	40.32	15.71	46.56	10.52
7	76.42	77.34	0.92	1.19	18.66	17.87	26.9	53.55	124.09	75.97
8	74.47	75.77	1.3	1.72	8.61	1.53	6.15	2.76	142.79	51.27
9	72.41	73.66	1.25	1.7	16.74	5.54	22.08	14.62	59.72	39.25
10	78.07	79.37	1.3	1.64	6.29	2.41	10.82	6.47	119.98	83.57
Average			0.99	1.31	12.49	8.36	30.04	20.70	95.98	39.61
Median			1.10	1.47	9.90	7.51	33.28	15.52	92.72	38.46

TABLE 4. Performance summary.

	HR (Averaged)		HRV (Averaged)
Experiment	AD_{HR} (bpm)	Accuracy (%)	AD_{SDNN} (ms)
Chest PPG vs Chest ECG	0.41	99.53	19.60
Chest PPG vs Finger PPG	0.84	98.95	12.80
Chest PPG vs Wrist PPG	0.99	98.69	12.49
CARMA	2.26	-	-
TROIKA	2.34	99.2[a]	-

a: Pearson correlation

AD was only 12.49 ms for all 10 subjects. It confirms that chest PPG is more accurate in measuring HR and HRV than wrist PPG. Also, both SpO_2 from the chest and wrist were extracted, demonstrating a standard deviation of 0.98%.

From all three experiments (seen in Table 4), chest PPG demonstrates an overall HR measurement accuracy of $> 98.6\,\%$ and a small HRV AD (Averaged AD_{SDNN} $\leq$19.6 ms) with robustness in ambulant scenarios when benchmarked with chest ECG and finger/wrist PPG in a 7-min protocol. A comparison has been made with other algorithms like TROIKA and CARMA, confirming the effectiveness of chest PPG measurement [56], [57].

V. CONCLUSION

This paper presents a first-of-its-kind exploration for measuring chest PPG with a custom system exhibiting high dynamic range. We successfully acquired the chest PPG signal and identified the best measurement region on the chest. A 7-mins protocol was designed to mimic and cover daily ambulant scenarios in a seated workplace environment. Using the chest ECG as a reference, the chest PPG system achieved an average HR error of 0.41 bpm, resulting in $>$ 99.5% measurement accuracy while only having 19.6 ms HRV AD SDNN with 6 subjects. We have also successfully compared the chest PPG setup with commercial finger PPG and wrist PPG in 10 subjects. Chest PPG achieved a maximum averaged HR error of 0.99 bpm (98.69% accuracy), and a maximum averaged HRV AD SDNN of 95.98 ms. In addition, respiration, another important biomedical parameter, was extracted, thereby presenting novel opportunities compared to conventional ECG and PPG modalities. Future work will extend our investigation toward chest PPG validation and involve more subjects and more activities to improve the database and reliability. This could provide insights into monitoring respiratory diseases such as early diagnosis of severe Covid cases. Lastly, future research would focus on the form factor miniaturization of the setup and integrate advanced algorithms within the processor on the custom ASIC platform to perform real-time measurement capabilities and improve accuracy.

REFERENCES

[1] C. D. Mathers, T. Boerma, and D. M. Fat, "Global and regional causes of death," *Brit. Med. Bull.*, vol. 92, no. 1, pp. 7–32, Dec. 2009.

[2] J. S. Ross et al., "Einthoven's string galvanometer," *Geriatrics*, vol. 53, no. 2, p. 89, 1998.

[3] A. Baranchuk et al., "Electromagnetic interference of communication devices on ECG machines," *Clin. Cardiol.*, vol. 32, no. 10, pp. 588–592, Oct. 2009.

[4] C. Van Mieghem, M. Sabbe, and D. Knockaert, "The clinical value of the ECG in noncardiac conditions," *Chest*, vol. 125, no. 4, pp. 1561–1576, Apr. 2004.

[5] S. Sarkar, P. Bhattacharyya, M. Mitra, and S. Pal, "Automatic detection of obstructive and restrictive lung disease from features extracted from ECG and ECG derived respiration signals," *Biomed. Signal Process. Control*, vol. 71, Jan. 2022, Art. no. 102791.

[6] K. A. Kaczmarek and J. G. Webster, "Voltage-current characteristics of the electrotactile skin-electrode interface," in *Proc. Annu. Int. IEEE Eng. Med. Biol. Soc.*, vol. 64, Seattle, WA, USA, Nov. 1989, pp. 1526–1527.

[7] Y. M. Chi, T.-P. Jung, and G. Cauwenberghs, "Dry-contact and noncontact biopotential electrodes: Methodological review," *IEEE Rev. Biomed. Eng.*, vol. 3, pp. 106–119, 2010.

[8] M. Chen et al., "A 400 GO input-impedance active electrode for non-contact capacitively coupled ECG acquisition with large linear-input-range and high CM-interference-tolerance," *IEEE Trans. Biomed. Circuits Syst.*, vol. 13, no. 2, pp. 376–386, Apr. 2019.

[9] R. R. Harrison and C. Charles, "A low-power low-noise CMOS amplifier for neural recording applications," *IEEE J. Solid-State Circuits*, vol. 38, no. 6, pp. 958–965, Jun. 2003.

[10] M. S. J. Steyaert and W. M. C. Sansen, "A micropower low-noise monolithic instrumentation amplifier for medical purposes," *IEEE J. Solid-State Circuits*, vol. SSC-22, no. 6, pp. 1163–1168, Dec. 1987.

[11] N. Van Helleputte et al., "A 345 μW multi-sensor biomedical SoC with bio-impedance, 3-channel ECG, motion artifact reduction, and integrated DSP," *IEEE J. Solid-State Circuits*, vol. 50, no. 1, pp. 230–244, Jan. 2015.

[12] J. Xu et al., "A 0.6 V 3.8 μW ECG/bio-impedance monitoring IC for disposable health patch in 40 nm CMOS," in *Proc. IEEE Custom Integr. Circuits Conf. (CICC)*, Apr. 2018, pp. 1–4.

[13] J. Xu, R. F. Yazicioglu, B. Grundlehner, P. Harpe, K. A. A. Makinwa, and C. Van Hoof, "A 160 μW 8-channel active electrode system for EEG monitoring," *IEEE Trans. Biomed. Circuits Syst.*, vol. 5, no. 6, pp. 555–567, Dec. 2011.

[14] Q. Lin et al., "Wearable multiple modality bio-signal recording and processing on chip: A review," *IEEE Sensors J.*, vol. 21, no. 2, pp. 1108–1123, Jan. 2021.

[15] R. Rawassizadeh, B. A. Price, and M. Petre, "Wearables: Has the age of smartwatches finally arrived?" *Commun. ACM*, vol. 58, no. 1, pp. 45–47, Jan. 2015.

[16] S. M. R. Islam, D. Kwak, M. H. Kabir, M. Hossain, and K. Kwak, "The Internet of Things for health care: A comprehensive survey," *IEEE Access*, vol. 3, pp. 678–708, 2015.

[17] J. Wei, "How wearables intersect with the cloud and the Internet of Things: Considerations for the developers of wearables," *IEEE Consum. Electron. Mag.*, vol. 3, no. 3, pp. 53–56, Jul. 2014.

[18] A. V. J. Challoner and C. A Ramsay, "A photoelectric plethysmograph for the measurement of cutaneous blood flow," *Phys. Med. Biol.*, vol. 19, no. 3, pp. 317–328, May 1974.

[19] A. B. Hertzman, "The blood supply of various skin areas as estimated by the photoelectric plethysmograph," *Amer. J. Physiol.-Legacy Content*, vol. 124, no. 2, pp. 328–340, 1938.

[20] P. H. Charlton, P. A. Kyriacou, J. Mant, V. Marozas, P. Chowienczyk, and J. Alastruey, "Wearable photoplethysmography for cardiovascular monitoring," *Proc. IEEE*, vol. 110, no. 3, pp. 355–381, Mar. 2022.

[21] *Pulse Oximetry Training Manual*, World Health Org., Geneva, Switzerland, 2011.

[22] M. A. O'Leary, "Imaging with diffuse photon density waves," Ph.D. dissertation, Dept. Phys., Univ. PA, Philadelphia, PA, USA, 1996.

[23] J. H. Lambert, *Photometria Sive De Mensura Et Gradibus Luminis, Colorum Et Umbrae*. Stuttgart, Germany: Klett, 1760.

[24] V. Beer, "Bestimmung der absorption des rothen lichts in farbigen flüssigkeiten," *Annalen der Physik*, vol. 162, no. 5, pp. 78–88, Jan. 1852.

[25] E. M. C. Hillman, "Experimental and theoretical investigations of near infrared tomographic imaging methods and clinical applications," Ph.D. dissertation, Univ. London, London, U.K., 2002.

[26] A. A. R. Kamal, J. B. Harness, G. Irving, and A. J. Mearns, "Skin photoplethysmography—A review," *Comput. Methods Programs Biomed.*, vol. 28, no. 4, pp. 257–269, 1989.

[27] J. Näslund, J. Pettersson, T. Lundeberg, D. Linnarsson, and L.-G. Lindberg, "Non-invasive continuous estimation of blood flow changes in human patellar bone," *Med. Biol. Eng. Comput.*, vol. 44, no. 6, pp. 501–509, Jun. 2006.

[28] (2014). *Osram-SFH 7050*. [Online]. Available: https://www.osram.com/Home/OptoSemiconductors/tech

[29] J. Allen, "Photoplethysmography and its application in clinical physiological measurement," *Physiol. Meas.*, vol. 28, no. 3, pp. R1–R39, Mar. 2007.

[30] (2017). *Maxim 6547, Using Reflectometry for a PPG Waveform*. [Online]. Available: https://www.maximintegrated.com

[31] Q. Lin et al., "A 119 dB dynamic range charge counting light-to-digital converter for wearable PPG/NIRS monitoring applications," *IEEE Trans. Biomed. Circuits Syst.*, vol. 14, no. 4, pp. 800–810, Aug. 2020, doi: 10.1109/TBCAS.2020.3001449.

[32] Q. Lin et al., "A 134 dB dynamic range noise shaping slope light-to-digital converter for wearable chest PPG applications," *IEEE Trans. Biomed. Circuits Syst.*, vol. 15, no. 6, pp. 1224–1235, Dec. 2021.

[33] Q. Lin, W. Sijbers, C. Avidikou, C. Van Hoof, F. Tavernier, and N. Van Helleputte, "Photoplethysmography (PPG) sensor circuit design techniques," in *Proc. IEEE Custom Integr. Circuits Conf. (CICC)*, Apr. 2022, pp. 1–8.

[34] D. Biswas et al., "CorNET: Deep learning framework for PPG-based heart rate estimation and biometric identification in ambulant environment," *IEEE Trans. Biomed. Circuits Syst.*, vol. 13, no. 2, pp. 282–291, Apr. 2019.

[35] L. Nilsson, T. Goscinski, S. Kalman, L. Lindberg, and A. Johansson, "Combined photoplethysmographic monitoring of respiration rate and pulse: A comparison between different measurement sites in spontaneously breathing subjects," *Acta Anaesthesiol. Scand.*, vol. 51, no. 9, pp. 1250–1257, Aug. 2007.

[36] M. Kramer, A. Lobbestael, E. Barten, J. Eian, and G. Rausch, "Wearable pulse oximetry measurements on the torso, arms, and legs: A proof of concept," *Mil. Med.*, vol. 182, pp. 92–98, Mar. 2017.

[37] A. Kiruthiga et al., "Reflectance pulse oximetry for blood oxygen saturation measurement from diverse locations—A preliminary analysis," in *Proc. IEEE Int. Symp. Med. Meas. Appl. (MeMeA)*, Jun. 2018, pp. 1–6.

[38] K. Zhu, M. Li, S. Akbarian, M. Hafezi, A. Yadollahi, and B. Taati, "Vision-based heart and respiratory rate monitoring during sleep—A validation study for the population at risk of sleep apnea," *IEEE J. Transl. Eng. Health Med.*, vol. 7, pp. 1–8, 2019.

[39] S. K. Longmore, G. Y. Lui, G. Naik, P. P. Breen, B. Jalaludin, and G. D. Gargiulo, "A comparison of reflective photoplethysmography for detection of heart rate, blood oxygen saturation, and respiration rate at various anatomical locations," *Sensors*, vol. 19, no. 8, p. 1874, Apr. 2019.

[40] *WHO Mild COVID-19 Homecare Bundle*, World Health Org., Geneva, Switzerland, 2022.

[41] K. Nakajima, T. Tamura, and H. Miike, "Monitoring of heart and respiratory rates by photoplethysmography using a digital filtering technique," *Med. Eng. Phys.*, vol. 18, pp. 365–372, Jul. 1996.

[42] Q. Lin et al., "A 28 μW 134dB DR 2nd-order noise-shaping slope light-to-digital converter for chest PPG monitoring," in *IEEE Int. Solid-State Circuits Conf. (ISSCC) Dig. Tech. Papers*, Feb. 2021, pp. 390–392.

[43] F. Marefat, R. Erfani, K. L. Kilgore, and P. Mohseni, "A 280 μW 108 dB DR readout IC with wireless capacitive powering using a dual-output regulating rectifier for implantable PPG recording," in *IEEE Int. Solid-State Circuits Conf. (ISSCC) Dig. Tech. Papers*, Feb. 2020, pp. 412–414.

[44] F. Marefat, R. Erfani, and P. Mohseni, "A 1-V 8.1-μW PPG-recording front-end with >92-dB DR using light-to-digital conversion with signal-aware DC subtraction and ambient light removal," *IEEE Solid-State Circuits Lett.*, vol. 3, pp. 17–20, 2020.

[45] *7050-Photoplethysmography Sensor*, OSRAM, SFH, Munich, Germany, 2016.

[46] D. Zhai, "Modeling of smoking behavior and lapse prediction using wearable and contextual sensors," KU Leven, Belgium, Rep. 3E160537, 2021.

[47] L. S. Lilly, *Pathophysiology of Heart Disease: A Collaborative Project of Medical Students and Faculty*. Baltimore, MD, USA: Williams & Wilkins, 2012.

[48] P. Van Gent, H. Farah, N. Nes, and B. van Arem, "Heart rate analysis for human factors: Development and validation of an open-source toolkit for noisy naturalistic heart rate data," in *Proc. 6th Humanist Conf.*, 2018, pp. 173–178.

[49] P. van Gent, T. Melman, H. Farah, N. van Nes, and B. van Arem, "Multi-level driver workload prediction using machine learning and off-the-shelf sensors," *Transp. Res. Rec., J. Transp. Res. Board*, vol. 2672, no. 37, pp. 141–152, Dec. 2018.

[50] P. van Gent, H. Farah, N. van Nes, and B. van Arem, "HeartPy: A novel heart rate algorithm for the analysis of noisy signals," *Transp. Res. F, Traffic Psychol. Behav.*, vol. 66, pp. 368–378, Oct. 2019.

[51] A. Golgouneh and B. Tarvirdizadeh, "Fabrication of a portable device for stress monitoring using wearable sensors and soft computing algorithms," *Neural Comput. Appl.*, vol. 32, no. 11, pp. 7515–7537, Jun. 2020.

[52] A. Schäfer and J. Vagedes, "How accurate is pulse rate variability as an estimate of heart rate variability? A review on studies comparing photoplethysmographic technology with an electrocardiogram," *Int. J. Cardiol.*, vol. 166, no. 1, pp. 15–29, 2013.

[53] S. S. Oak and P. Aroul, "How to design peripheral oxygen saturation (SpO_2) and optical heart rate monitoring (OHRM) systems using the AFE 4403," Texas Instrum., TX, USA, Rep. SLAA655, 2015.

[54] K. Rogoza and W. Kosiak, "Usefulness of lung ultrasound in diagnosing causes of exacerbation in patients with chronic dyspnea," *Adv. Respiratory Med.*, vol. 84, no. 1, pp. 38–46, Dec. 2015.

[55] *American National Standard: Cardiac Monitors, Heart Rate Meters, and Alarms (ANSI/AAMI EC13)*, Assoc. for Advancement Med. Instrum., Arlington, VA, USA, 2002.

[56] Z. Zhang, "Photoplethysmography-based heart rate monitoring in physical activities via joint sparse spectrum reconstruction," *IEEE Trans. Biomed. Eng.*, vol. 62, no. 8, pp. 1902–1910, Aug. 2015.

[57] A. Bacà et al., "CARMA: A robust motion artifact reduction algorithm for heart rate monitoring from PPG signals," in *Proc. 23rd Eur. Signal Process. Conf. (EUSIPCO)*, Nice, France, Aug. 2015, pp. 2646–2650.